nature COMMUNICATIONS

ARTICLE

Received 14 Jan 2013 | Accepted 9 May 2013 | Published 13 Jun 2013

DOI: 10.1038/ncomms2998 OPEN

Carbon dioxide concentration dictates alternative methanogenic pathways in oil reservoirs

Daisuke Mayumi[1], Jan Dolfing[2], Susumu Sakata[1], Haruo Maeda[3], Yoshihiro Miyagawa[3], Masayuki Ikarashi[3], Hideyuki Tamaki[4], Mio Takeuchi[1], Cindy H. Nakatsu[5] & Yoichi Kamagata[4,6]

Deep subsurface formations (for example, high-temperature oil reservoirs) are candidate sites for carbon capture and storage technology. However, very little is known about how the subsurface microbial community would respond to an increase in CO_2 pressure resulting from carbon capture and storage. Here we construct microcosms mimicking reservoir conditions (55 °C, 5 MPa) using high-temperature oil reservoir samples. Methanogenesis occurs under both high and low CO_2 conditions in the microcosms. However, the increase in CO_2 pressure accelerates the rate of methanogenesis to more than twice than that under low CO_2 conditions. Isotope tracer and molecular analyses show that high CO_2 conditions invoke acetoclastic methanogenesis in place of syntrophic acetate oxidation coupled with hydrogenotrophic methanogenesis that typically occurs in this environment (low CO_2 conditions). Our results present a possibility of carbon capture and storage for enhanced microbial energy production in deep subsurface environments that can mitigate global warming and energy depletion.

[1] Institute for Geo-Resources and Environment, National Institute of Advanced Industrial Science and Technology (AIST), 1-1-1 Higashi, Tsukuba 305-8567, Japan. [2] School of Civil Engineering and Geosciences, Newcastle University, Newcastle upon Tyne NE1 7RU, UK. [3] INPEX Corporation, 5-3-1 Akasaka, Minato-ku 107-6332, Japan. [4] Bioproduction Research Institute, National Institute of Advanced Industrial Science and Technology (AIST), 1-1-1 Higashi, Tsukuba 305-8566, Japan. [5] Department of Agronomy, Purdue University, West Lafayette, Indiana 47907, USA. [6] Bioproduction Research Institute, National Institute of Advanced Industrial Science and Technology (AIST), Toyohira, Sapporo 062-8517, Japan. Correspondence and requests for materials should be addressed to S.S. (email: su-sakata@aist.go.jp) or to Y.K. (email: y.kamagata@aist.go.jp)

Carbon capture and storage (CCS) is a candidate technology to reduce the emission of CO_2 from factories and power plants[1,2]. The underlying idea is to capture CO_2 rather than emitting it into the atmosphere and to sequester it in deep subsurface formations such as deep saline aquifers or depleted oil and gas reservoirs[3]. This technology has the potential to reduce future global CO_2 emissions by 20%[2,4]. The economical and technological feasibilities of CCS have been extensively studied over the past decade, mainly from a geological perspective[5–8]. Recently, microbial effects associated with CO_2 storage also have been investigated in deep saline aquifers[9,10], and the influence of CO_2 injection on microbial community structure has been reported. A study revealed that CO_2 injection changed the constituent of methanogens and sulfate reducers in the deep subsurface microbial community[10]. Oil reservoirs are also unique subsurface environments that are potential repositories for CO_2 sequestration[11,12] and often harbor active methane-producing microbial communities[13–15]. However, very little is known about the effect of CO_2 sequestration on microbial communities and their functional role in deep subsurface oil reservoirs.

In the present study, we aimed to reveal how the microbial community and functions associated with methanogenesis respond to the increase in CO_2 concentration in the oil reservoirs. We performed laboratory experiments that simulated field conditions from where samples were collected. Based on stable isotope tracer analysis, molecular analysis and thermodynamic calculations, we report the possibility that drastic changes of microbial communities and methanogenic functions can be induced by CO_2 injection into deep subsurface high-temperature oil reservoirs.

Results

Effect of CO_2 on methanogenesis in oil field microcosms. We selected a high-temperature oil reservoir, Yabase oil field, Japan, where we previously demonstrated the occurrence of *in situ* methanogenic activity[15]. Acetate, which is highly abundant in this reservoir (6–9 mM), is a primary precursor to methane. We previously found that methane was produced from acetate via syntrophic acetate oxidation coupled with hydrogenotrophic methanogenesis in the reservoir[15]. To determine if methanogenesis would continue if CO_2 concentrations increased in subsurface oil reservoirs, we set up high-temperature and high-pressure incubation apparatuses (working volume: 1 l; Supplementary Fig. S1), mimicking the *in situ* oil reservoir (1,000–1,300 m deep, 53–65 °C, 5 MPa; Supplementary Table S1). Production water from the reservoir used in this study contained 6.4 mM of acetate, 39.6 mM of bicarbonate and indigenous microbes. We inoculated 8 ml of crude oil and 800 ml of the production water as a source of indigenous microbes and nutrients into the apparatuses, pressurized with either N_2 or N_2/CO_2 (90:10) gas to a final pressure of 5 MPa, and incubated at 55 °C. The microcosms incubated under an N_2 atmosphere were designated 'control microcosms', and those incubated under an N_2/CO_2 atmosphere were designated as 'CO_2-injected microcosms'. Control and CO_2-injected microcosm experiments were prepared in triplicate. Two of the three microcosms were amended with either a trace amount of ^{13}C-bicarbonate (final 400 μM) or [2-^{13}C]-acetate (final 87.5 μM) to track the methanogenic pathway.

After 1 week of incubation, CO_2 partial pressures and bicarbonate concentrations in the control microcosms stabilized at ~0.004 MPa (=0.04 atm) and 47.7 mM and in the CO_2-injected microcosms at 0.2 MPa (=2.0 atm) and 86.4 mM; decrease in CO_2 was due to dissolution into the production water. The pH levels in both microcosms were stable at ~8.2 and 7.3, respectively, during incubation. The conditions in the

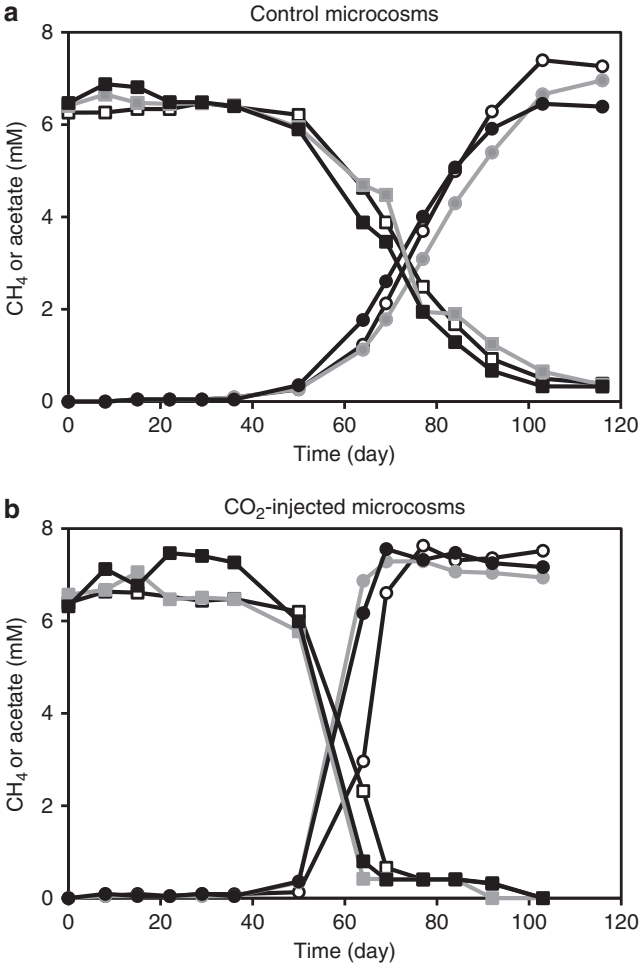

Figure 1 | Methanogenesis in control and CO_2-injected microcosms. Methanogenesis shown in (**a**) three individual control microcosms and (**b**) three individual CO_2-injected microcosms under high-temperature and high-pressure conditions (55 °C and 5 MPa). Methane (circles) and acetate (squares) concentrations over time in the unlabeled (closed symbols), [2-^{13}C]-acetate (gray symbols) and ^{13}C-bicarbonate (open symbols)-labeled microcosms. All six microcosms were constructed using high-temperature oil reservoir samples.

CO_2-injected microcosms were likely to reflect the bicarbonate concentration and pH in previously reported CCS sites (Supplementary Table S1). In all microcosms, methane productions increased after at least 50 days of incubation, whereas methane productions in CO_2-injected microcosms completed ~30 days earlier than the control microcosms (Fig. 1a,b). Acetate present in the original production water decreased concomitantly with increased methane production. Methane production and acetate degradation in microcosms labeled with stable isotope tracers were almost similar to unlabeled microcosms. Methane production was nearly equivalent to the acetate consumed. This stoichiometric methanogenic reaction suggests that almost all the methane formed was derived from acetate. Interestingly, the methane production rate in CO_2-injected microcosms (0.36 ± 0.04 μmol d^{-1} ml^{-1} water at the growing phase) was twice as high as in control microcosms (0.17 ± 0.02 μmol d^{-1} ml water at the growing phase), indicating that CO_2 injection stimulated methanogenesis.

CO_2-driven change in methanogenic pathway in microcosms. To identify the methanogenic pathways in the control and

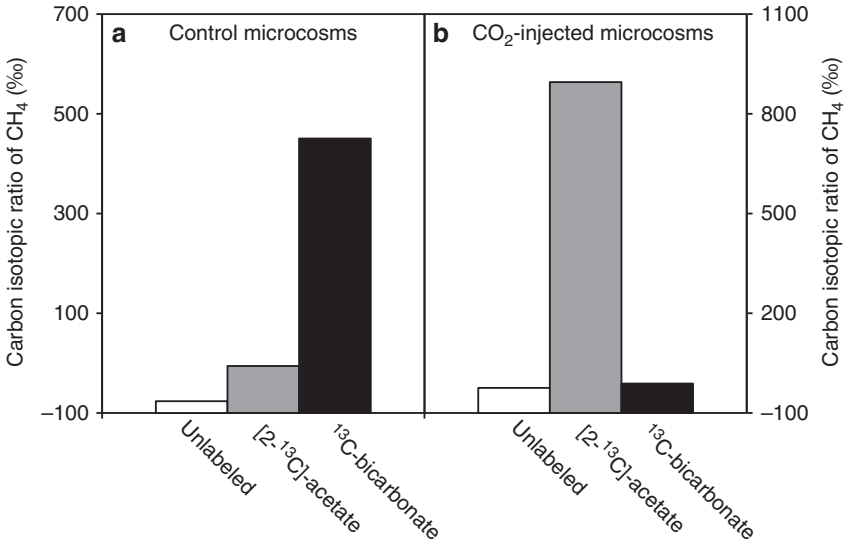

Figure 2 | Carbon isotopic ratios of methane in control and CO_2-injected microcosms after incubation. Carbon isotopic ratios of methane in the (**a**) control microcosms and (**b**) CO_2-injected microcosms after incubation of 103 days. Carbon isotopic ratios of methane and dissolved inorganic carbon (DIC) in each microcosm during incubation are shown in Supplementary Table S2.

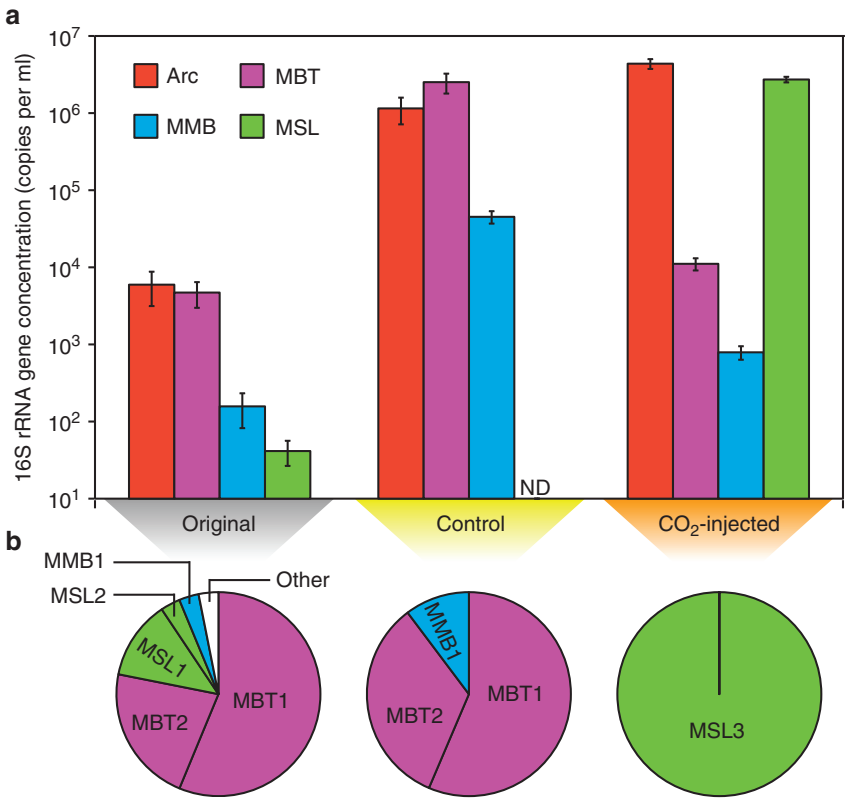

Figure 3 | Archaeal methanogenic community compositions. Archaeal methanogenic community compositions in the original production water, control (day 116) and CO_2-injected microcosms (day 103). (**a**) The 16S rRNA gene copy concentrations of the domain *Archaea* (Arc), the orders *Methanobacteriales* (MBT), *Methanomicrobiales* (MMB), and *Methanosarcinales* (MSL) quantified by qPCR assays. ND, not detected. (**b**) Relative abundance of archaeal clones. MBT1: *Methanothermobacter thermautotrophicus* KZ3-1 (DQ657903) (>99% similarity), MBT2: *Methanothermobacter wolfeii* KZ24a (DQ657904) (>95% similarity), MSL1: *Methanosaeta* sp. (AJ133791) (99% similarity), MSL2: *Methanolobus psychrophilus* R15 (EF202842) (98% similarity), MSL3: *Methanosaeta thermophila* PT (AB071701) (99% similarity), MMB1: *Methanoculleus receptaculi* ZC-3 (DQ787475) (99% similarity), Other: *Thermococcus litoralis* DSM5474 (AY099180) (99% similarity). Details of archaeal clone library analysis are shown in Supplementary Table S4.

CO_2-injected microcosms, the carbon isotopic compositions ($\delta^{13}C$) of methane and dissolved inorganic carbon (DIC) were measured during incubation. In the control microcosms labeled with ^{13}C-bicarbonate, elevated $\delta^{13}C$ methane values (>450‰) were detected (Fig. 2a), showing that the amended ^{13}C-bicarbonate was converted to $^{13}CH_4$. In the [2-^{13}C]-acetate-labeled

control microcosm, $\delta^{13}C_{DIC}$ values gradually increased and methane also became enriched in ^{13}C following DIC (Supplementary Table S2), indicating that the ^{13}C-methyl group of acetate was oxidized to CO_2 and incorporated into a large CO_2 pool, and a small fraction of $^{13}CO_2$ was converted to $^{13}CH_4$ (acetate oxidation: $CH_3COO^- + H^+ + 2H_2O \rightarrow 4H_2 + 2CO_2$; methanogenesis from H_2: $4H_2 + CO_2 \rightarrow CH_4 + 2H_2O$; over all, $CH_3COO^- + H^+ \rightarrow CH_4 + CO_2$). In contrast, the [2-$^{13}C$]-acetate added to a CO_2-injected microcosm resulted in elevated $\delta^{13}C$ methane values (>850‰) (Fig. 2b). This indicates that the ^{13}C-methyl group of acetate was directly converted to $^{13}CH_4$ ($^{13}CH_3COO^- + H^+ \rightarrow {}^{13}CH_4 + CO_2$). These observations demonstrated that the dominant methanogenic pathway in the control microcosms was syntrophic acetate oxidation coupled with hydrogenotrophic methanogenesis, while acetoclastic methanogenesis was the dominant methanogenic pathway in the CO_2-injected microcosms. The values of carbon isotopic fractionation between CH_4 and DIC in the unlabeled control ($\varepsilon_C = -83.3 \pm 1.3$‰) and CO_2-injected ($\varepsilon_C = -10.9 \pm 1.0$‰) microcosms during incubation (Supplementary Table S2) were also consistent with the hydrogenotrophic and acetoclastic methanogenesis, respectively[16]. The reproducibility of the impact of CO_2 on the methanogenic pathway and community resiliency were confirmed by an additional stable isotope tracer experiment, which showed that the dominant methanogenic community and pathway switched from one to the other when the headspace gas of the control microcosm was replaced with N_2/CO_2 (90:10) and the CO_2-injected microcosm was replaced with 100% N_2 (Supplementary Note 1; Supplementary Figs. S2 and S3, and Supplementary Tables S3, S4 and S5).

CO_2-induced alteration of methanogenic microbial community. Quantitative PCR (qPCR) and 16S rRNA gene clone library analysis showed differences in microbial community structure in the original production water compared with the incubated microcosms. The qPCR assays (Fig. 3a) of the archaeal 16S rRNA genes showed that (1) the original production water contained mostly the order *Methanobacteriales* and a smaller population of *Methanosarcinales*; (2) the control microcosm was similarly dominated by hydrogenotrophic methanogens affiliated with the order *Methanobacteriales*; whereas (3) the CO_2-injected microcosms differed and were dominated by the order *Methanosarcinales*, many of which are acetoclastic methanogens. Clone library analyses supported the qPCR results. In the original production water and control microcosm, the genus *Methanothermobacter* dominated the archaeal community (Fig. 3b and Supplementary Table S4). The control microcosm bacterial community was dominated by a limited number of phylotypes that includes the genus *Thermacetogenium*[17], a known syntrophic acetate-oxidizing bacterium (99.8% sequence similarity) (Supplementary Table S5). In contrast, all archaeal clones in the CO_2-injected microcosms were affiliated with the acetoclastic species *Methanosaeta thermophila* strain PT (99% sequence similarity) (Fig. 3b and Supplementary Table S4). In addition, in the CO_2-injected microcosms, heterotrophic fermentative bacteria such as *Coprothermobacter proteolyticus* dominated in the bacterial community and the known syntrophic acetate-oxidizing bacteria disappeared (Supplementary Table S5). These results clearly demonstrated that the main constituents of the control microcosm methanogenic microbial community were hydrogenotrophic methanogens and syntrophic acetate-oxidizers; CO_2 injection changed the community and led to the dominance of acetoclastic methanogens. These findings are consistent with the change in methanogenic pathways assessed by the stable isotope tracer experiment.

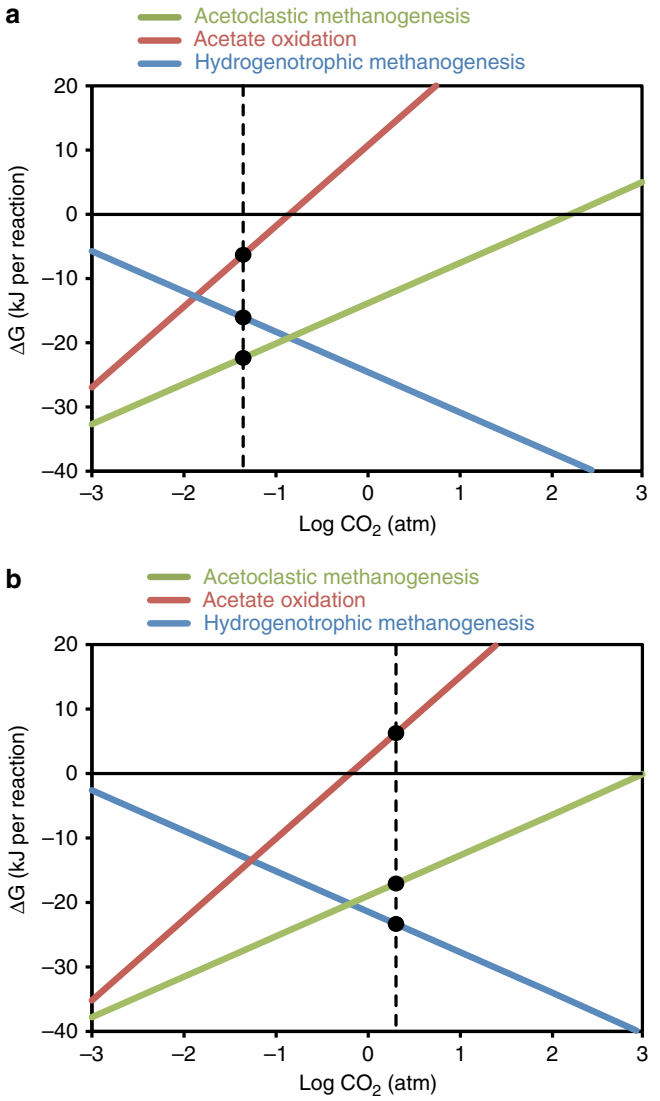

Figure 4 | CO_2 partial pressure effect on change in Gibbs free energy for acetate oxidation and methanogeneses. Effect of CO_2 partial pressure on the change in Gibbs free energy for acetate oxidation, hydrogenotrophic methanogenesis and acetoclastic methanogenesis. (**a**) The setup conditions are at 116 days of incubation in the control microcosm: acetate at 0.3 mM, methane at 0.51 atm, hydrogen at 1.5×10^{-4} atm, pH = 8.1, at 55 °C and 50 atm. (**b**) The setup conditions are at 77 days of incubation in the CO_2-injected microcosm: acetate at 0.4 mM, methane at 0.66 atm, hydrogen at 1.2×10^{-4} atm, pH = 7.3, at 55 °C and 50 atm. Dashed lines indicate actual CO_2 partial pressures (0.04 and 2.0 atm) in the control and CO_2-injected microcosms, respectively.

Thermodynamic constraints on methanogenic reactions. To elucidate the underpinning mechanisms of the shift in methanogenic pathways in conjunction with microbial community transition by injecting CO_2, we conducted thermodynamic calculations for the following reactions under various partial pressures of CO_2: acetate oxidation, hydrogenotrophic methanogenesis and acetoclastic methanogenesis. The thermodynamics showed that hydrogenotrophic methanogenesis becomes energetically more favorable with increasing CO_2 partial pressure, whereas acetate oxidation and acetoclastic methanogenesis become less favorable (Fig. 4a,b). However, acetoclastic methanogenesis is less sensitive to high CO_2 partial pressure than acetate oxidation because acetate oxidation produces two moles of

Table 1 | Thermodynamic parameters and Gibbs free energies of three reactions in the control and CO_2-injected microcosms.

Reaction	ΔH^o (kJ)	ΔG^o (kJ)	$\Delta G^o_{55,\ 1}$ (kJ)*	$\Delta G^o_{55,\ 50}$ (kJ)*	$\Delta G_{55,\ 50}$ (kJ)†	
					Control	CO_2-injected
Acetoclastic methanogenesis ($CH_3COO^- + H^+ \rightarrow CH_4 + CO_2$)	17.7	−75.8	−85.2	−85.0	−22.4	−17.1
Acetate oxidation ($CH_3COO^- + H^+ + 2H_2O \rightarrow 4H_2 + 2CO_2$)	270.6	55.0	33.3	33.8	−6.3	6.1
Hydrogenotrophic methanogenesis ($4H_2 + CO_2 \rightarrow CH_4 + 2H_2O$)	−252.9	−130.8	−118.5	−118.8	−16.1	−23.1

*The Gibbs free energies, $\Delta G^o_{55,\ 1}$ and $\Delta G^o_{55,\ 50}$, were calculated under the conditions at 55 °C and 1 atm, and at 55 °C and 50 atm, respectively.
†The Gibbs free energies in the control and CO_2-injected microcosms were calculated using actual conditions in the unlabeled microcosms at day 116 and 77 of the control and CO_2-injected microcosms, respectively, at 55 °C and 50 atm.

CO_2 per mole of acetate, whereas acetoclastic methanogenesis produces one mole of CO_2. The ΔG values calculated for the three reactions in the control and CO_2-injected microcosms showed that acetate oxidation in the CO_2-injected microcosm would be endergonic (Fig. 4a,b and Table 1), indicating that syntrophic acetate oxidation coupled with hydrogenotrophic methanogenesis could not proceed under high CO_2 partial pressures but acetoclastic methanogenesis could proceed. A cultivation experiment verified the effect of CO_2 partial pressure on microbes; a pure syntrophic defined coculture[17] of *Thermacetogenium phaeum* strain PB and *Methanothermobacter thermoautotrophicus* strain TM was also inhibited by increasing CO_2 partial pressure (Supplementary Note 2 and Supplementary Fig. S4).

Discussion

This study illustrates the possibility that an increase in CO_2 partial pressure will change the microbial ecosystem in a deep subsurface high-temperature oil reservoir. Our results suggest that CO_2 injection into deep subsurface oil reservoirs can alter the *in situ* methanogenic pathway and lead to the dominance of acetoclastic methanogenesis. Acetate is often the most abundant organic acid in oil reservoirs[18,19] and an important intermediate in methanogenesis from crude oil[20]. Given that acetoclastic methanogenesis generally leads to a faster methanogenic reaction than syntrophic acetate oxidation coupled to hydrogenotrophic methanogenesis (Supplementary Note 2 and Supplementary Fig. S4), the shift to this pathway may result in an acceleration of methane production in oil reservoirs as observed in this study (Fig. 1a,b). Furthermore, the thermodynamics, in theory, suggests that the shift to acetoclastic methanogenesis can ease the thermodynamic constraint of crude oil biodegradation (Supplementary Fig. S5). Perhaps, the largest window of opportunity for crude oil biodegradation via acetoclastic methanogenesis alone[21] may lend further support to the hypothesis that CCS may increase energy recovery in the form of methane through crude oil biodegradation. Our results present a possibility of CCS for enhanced microbial energy production in deep subsurface environments that can mitigate global warming and energy depletion at the same time. To date, very little is known about the influence of CO_2 sequestration on the subsurface microbial communities and their functions, despite their important contribution to global biogeochemical processes[22,23]. This study would intrigue not only geochemists but also microbiologists for further investigation of CCS in connection with utilization of microbial activities in deep subsurface.

Methods

Study site and sampling. Yabase oil field is one of the oldest and largest onshore oil fields in Japan, located in Akita Prefecture (39° 42′N, 140° 5′E). Currently, the oil field is almost depleted and characterized by high overall water cut (~90% basic sediment and water). The main reservoir rocks are tuffaceous sandstone of Miocene–Pliocene age. The depth of the oil horizon ranges from 1000 to 1300 m, with *in situ* temperature and pressure estimated to be 53–65 °C and 5 MPa, respectively.

In Yabase oil field, there are some production wells in which crude oil along with production water has been produced by pumping. In this study, reservoir samples were collected from one of the wells where water injection to enhance oil recovery has never been applied. The samples were taken from production flow at the wellhead by discharging the fluid mixture through a metal tube into gas-tight glass bottles flushed in advance with nitrogen gas in September 2009. Immediately before each bottle was sealed, the headspace was flushed and pressurized with nitrogen gas to minimize air contamination. The samples were maintained at 50°C for 3 days until use.

Geochemical characteristics of the production water and gas sample from this reservoir have been previously described in the study by Mayumi *et al.*[15] Briefly, the water had low salinity (Cl^-; 4690 mg l^{-1}) and −239 mV of reduction potential, and concentrations of nitrate and sulfate as electron acceptors were 14.5 μM and below 0.5 mM, respectively. Gas compositions of the sample collected from the production flow were H_2: 0.1%, CO_2: 2.4%, CH_4: 77.2%, C_2H_6: 10.8%, C_3H_8: 5.2%, *i*-C_4H_{10}: 0.8% and *n*-C_4H_{10}: 1.5%.

Microcosms. Six microcosms were prepared with 800 ml of production water and 8 ml of crude oil in 1 l sterile stainless-steel cylinder bottles (304L-HDF4-1000; Swagelok, Ohio, USA) and stable isotope tracers were added as described in Supplementary Fig. S1. Control microcosms were pressurized with nitrogen gas, and CO_2-injected microcosms were pressurized with N_2/CO_2 (90:10; $\delta_{CO2} = -34.8$‰) at 5 MPa. Before pressurization of CO_2-injected microcosms, sodium bicarbonate ($\delta_{NaHCO3} = -4.2$‰) was added to a final concentration of 74 mM to mimic *in situ* conditions where formation water is highly buffered due to the presence of minerals such as calcite ($CaCO_3$) and dolomite ($CaMg(CO_3)_2$) in oil reservoirs[9,12]. The microcosms were incubated at 55 °C, and the mixing ratios of CH_4 and CO_2 in the headspace gases and organic acids in production water were periodically measured with a gas chromatograph and an ion chromatograph[15]. H_2 concentrations in the headspace gases were measured with an EAGanalyzer gas chromatograph equipped with a semiconductor detector (Sensortec Co., Ltd., Shiga, Japan).

Carbon isotope analysis. Headspace gas and the incubated water were collected into gas-tight glass cylinder bottles and vials, respectively, from all microcosms periodically. Carbon isotopic compositions of CH_4 in gas-tight glass cylinder bottles were determined with a Finnigan gas chromatograph combustion isotope ratio mass spectrometer (GC-C-IRMS) consisting of a Hewlett Packard 5890 GC, a Finnigan MAT 252 IRMS and a ThermoQuest combustion interface (Thermo Finnigan Inc., Texas, USA). Carbon isotopic composition of DIC in the incubated water was measured after the addition of 1 M H_2SO_4 to liberate total CO_2. All measurements were conducted in triplicate, and the s.e. values were less than 1‰. The isotopic values were expressed in δ notation relative to the Vienna Pee Dee Belemnite (VPDB) standard. The values of isotopic fractionation (ε_C) between DIC and CH_4 were determined by $\varepsilon_C = (\delta_{CH4} - \delta_{DIC})/(1 + \delta_{DIC}/10^3)$.

Molecular biological analyses. Molecular analyses were carried out for the original production water and incubated water from [2-^{13}C]-acetate labeled microcosms (at day 116 and 103 for the control and the CO_2-injected microcosms, respectively). Total DNA was extracted from a 0.22-μm-pore-size polycarbonate membrane filter (Millipore, MA, USA), concentrating 250 ml of the original production water, 15 ml of the control microcosm water and 40 ml of the CO_2-injected microcosm water, using a FastDNA Spin kit (MP Biomedicals, CA, USA) according to the manufacturer's protocol. Bacterial and archaeal 16S rRNA genes were amplified with primer sets Eub8F/Univ1490R[24] and Ar109F[25]/Univ1490R, respectively. PCR products were cloned using the pT7 Blue T-vector kit (Novagen, CA, USA). Clones were randomly selected (in archaeal libraries, original production water; 32 clones, control microcosm; 39 clones, CO_2-injected microcosm; 35 clones, in bacterial libraries, original production water; 49 clones, control microcosm; 92 clones, CO_2-injected microcosm; 84 clones), and the inserted 16S rRNA gene was directly amplified with T7 promoter primer and U-19mer primer (Novagen). Sequence analysis of 16S rRNA genes was carried out with a BigDye Version 3.1 reaction on an ABI3730xl DNA Analyzer (Applied Biosystems, CA, USA). Chimeric sequences were detected with the Bellerophon server[26] and removed from the sequence data sets. To group the OTUs and draw

rarefaction curves, sequences were analyzed using FastGroupII program[27] with 97% sequence similarity. Representative sequences from each OTU were compared with those in public databases using the Seqmatch program from the Ribosomal Database Project (Release 10, Update 12) to identify the nearest neighbors.

The specific primer and probe set for archaea, hydrogenotrophic methanogens (the orders *Methanobacteriales* and *Methanomicrobiales*), and acetoclastic methanogens (the order *Methanosarcinales*) used in quantitative real-time PCR to determine the 16S rRNA gene copy numbers were previously designed in the study by Yu *et al.*[28] All real-time PCR assays were performed with iCycler iQ using the iQ Supermix reaction kit (Bio-Rad, California, USA), as previously described in the study by Mayumi *et al.*[15] Standard curves for each assay were constructed using nearly full-length 16S rRNA gene fragments amplified from *Methanothermobacter thermautotrophicus* strain delta H (DSM 1053) for the *Archaea* and the *Methanobacteriales* assays, *Methanoculleus bourgensis* strain MS2 (DSM3045) for the *Methanomicrobiales* assay, *Methanosaeta thermophila* strain PT (DSM 6194) for the *Methanosarcinales* assay.

Thermodynamics calculations. Gibbs free energy calculations were made according to the study by Dolfing *et al.*[21] Temperature corrections were made with the Gibbs–Helmholz equation according to $\Delta G^{o}_{Tact} = \Delta G^{o}_{Tref} \cdot (T_{act}/T_{ref}) + \Delta H^{o}_{Tref} \cdot (T_{ref} - T_{act})/T_{ref}$ with T in K; $T_{act} = 328.15$ K, $T_{ref} = 298.15$ K. The effect of pressure on ΔG (in kJ per reaction) was approximated as $\Delta G^{o}_{Tref,Pact} = \Delta G^{o}_{Tref,Pref} + \Delta V^{o} \cdot (P_{act} - P_{ref})/10000$ where $\Delta G^{o}_{Tref,Pact}$ is the Gibbs free energy of reaction at the reference temperature (298.15 K) and *in situ* pressure (5 MPa; 50 atm), $\Delta G^{o}_{Tref,Pref}$ is the standard Gibbs free energy of reaction at the reference temperature and pressure (0.1 MPa; 1 atm), P_{act} is the *in situ* pressure in atm, P_{ref} is the reference pressure in atm and ΔV^{o} is the partial molar volume change of the reaction at the reference temperature and pressure in $cm^3\ mol^{-1}$, as outlined in the study by Wang *et al.*[29]. The calculations were made for acetate ($pKa = 4.75$) at the appropriate pH values[30]. For the reaction $CO_2 + 4H_2 \rightarrow CH_4 + 2H_2O$, $\Delta V^{o} = -62.3$; for $CH_3COO^- + H^+ + 2H_2O \rightarrow 4H_2 + 2CO_2$, $\Delta V^{o} = 92.25$; for $CH_3COO^- + H^+ \rightarrow CH_4 + CO_2$, $\Delta V^{o} = 29.95$. Neglecting activity coefficients yields an error in calculated Gibbs free energy values of at most $2\ kJ\ mol^{-1}$ for all reported values at an ionic strength of 0.1 M (Debye–Huckel calculations).

References

1. Schrag, D. P. Preparing to capture carbon. *Science* **315,** 812–813 (2007).
2. Haszeldine, R. S. Carbon capture and storage: how green can black be? *Science* **325,** 1647–1652 (2009).
3. Metz, B., Davidson, O., de Coninck, H. C., Loos, M. & Meyer, L. A. *IPCC Special Report on Carbon Dioxide Captuer and Storage* (Cambridge University Press, 2005).
4. International Energy Agency. *Energy Technology Perspectives 2008* (International Energy Agency, Paris, 2008).
5. Lackner, K. S. *et al.* The urgency of the development of CO_2 capture from ambient air. *Proc. Natl Acad. Sci. USA* **109,** 13156–13162 (2012).
6. Wilson, E. J., Johnson, T. L. & Keith, D. W. Regulating the ultimate sink: managing the risks of geologic CO_2 storage. *Environ. Sci. Technol.* **37,** 3476–3483 (2003).
7. Bruant, R. G., Guswa, A. J., Celia, M. A. & Peters, C. A. Safe storage of CO_2 in deep saline aquifers. *Environ. Sci. Technol.* **36,** 240A–245A (2002).
8. House, K. Z. *et al.* Economic and energetic analysis of capturing CO_2 from ambient air. *Proc. Natl Acad. Sci. USA* **108,** 20428–20433 (2011).
9. Kirk, M. F. Variation in energy available to populations of subsurface anaerobes in response to geological carbon storage. *Environ. Sci. Technol* **45,** 6676–6682 (2011).
10. Morozova, D. *et al.* Monitoring of the microbial community composition in saline aquifers during CO_2 storage by fluorescence *in situ* hybridisation. *Int. J. Greenh. Gas Control* **4,** 981–989 (2010).
11. Ravagnani, A. G., Ligero, E. L. & Suslick, S. B. CO_2 sequestration through enhanced oil recovery in a mature oil field. *J. Petrol. Sci. Eng.* **65,** 129–138 (2009).
12. Hirsche, K. *et al.* in *IEA GHG Weyburn CO2 Monitoring & Storage Project Summary Report 2000–2004* Vol. 3 (eds Wilson, M. & Monea, M.) 73–148 (Petroleum Technology Research Centre, Regina, 2004).
13. Magot, M., Ollivier, B. & Patel, B. K. C. Microbiology of petroleum reservoirs. *Antonie Van Leeuwenhoek* **77,** 103–116 (2000).
14. Gieg, L. M., Davidova, I. A., Duncan, K. E. & Suflita, J. M. Methanogenesis, sulfate reduction and crude oil biodegradation in hot Alaskan oilfields. *Environ. Microbiol.* **12,** 3074–3086 (2010).
15. Mayumi, D. *et al.* Evidence for syntrophic acetate oxidation coupled to hydrogenotrophic methanogenesis in the high-temperature petroleum reservoir of Yabase oil field (Japan). *Environ. Microbiol* **13,** 1995–2006 (2011).
16. Fey, A., Claus, P. & Conrad, R. Temporal change of ^{13}C-isotope signatures and methanogenic pathways in rice field soil incubated anoxically at different temperatures. *Geochim. Cosmochim. Acta* **68,** 293–306 (2004).
17. Hattori, S., Kamagata, Y., Hanada, S. & Shoun, H. *Thermacetogenium phaeum* gen. nov., sp. nov., a strictly anaerobic, thermophilic, syntrophic acetate-oxidizing bacterium. *Int. J. Syst. Evol. Microbiol.* **50,** 1601–1609 (2000).
18. Barth, T. Organic acids and inorganic ions in waters from petroleum reservoirs, Norwegian continental shelf: a multivariate statistical analysis and comparison with American reservoir formation waters. *Appl. Geochem* **6,** 1–15 (1991).
19. Barth, T. & Riis, M. Interactions between organic acid anions in formation waters and reservoir mineral phases. *Org. Geochem.* **19,** 455–482 (1992).
20. Jones, D. M. *et al.* Crude oil biodegradation via methanogenesis in subsurface petroleum reservoirs. *Nature* **451,** 176–180 (2008).
21. Dolfing, J., Larter, S. R. & Head, I. M. Thermodynamic constraints on methanogenic crude oil biodegradation. *ISME J.* **2,** 442–452 (2008).
22. Pedersen, K. The deep subterranean biosphere. *Earth Sci. Rev.* **34,** 243–260 (1993).
23. Whitman, W. B., Coleman, D. C. & Wiebe, W. J. Prokaryotes: the unseen majority. *Proc. Natl Acad. Sci. USA* **95,** 6578–6583 (1998).
24. Weisburg, W. G., Barns, S. M., Pelletier, D. A. & Lane, D. J. 16S ribosomal DNA amplification for phylogenetic study. *J. Bacteriol.* **173,** 697–703 (1991).
25. Imachi, H. *et al.* Non-sulfate-reducing, syntrophic bacteria affiliated with *Desulfotomaculum* cluster I are widely distributed in methanogenic environments. *Appl. Environ. Microbiol.* **72,** 2080–2091 (2006).
26. Huber, T., Faulkner, G. & Hugenholtz, P. Bellerophon: a program to detect chimeric sequences in multiple sequence alignments. *Bioinformatics.* **20,** 2317–2319 (2004).
27. Yu, Y. N., Breitbart, M., McNairnie, P. & Rohwer, F. FastGroupII: a web-based bioinformatics platform for analyses of large 16S rDNA libraries. *BMC Bioinformatics* **7,** 57 (2006).
28. Yu, Y., Lee, C., Kim, J. & Hwang, S. Group-specific primer and probe sets to detect methanogenic communities using quantitative real-time polymerase chain reaction. *Biotechnol. Bioeng.* **89,** 670–679 (2005).
29. Wang, G. Z., Spivack, A. J. & D'Hondt, S. Gibbs energies of reaction and microbial mutualism in anaerobic deep subseafloor sediments of ODP Site 1226. *Geochim. Cosmochim. Acta* **74,** 3938–3947 (2010).
30. Dolfing, J., Xu, A. P. & Head, I. M. Anomalous energy yields in thermodynamic calculations: importance of accounting for pH-dependent organic acid speciation. *ISME J.* **4,** 463–464 (2010).

Acknowledgements

We gratefully acknowledge the Akita District Office of INPEX Corporation for their help with sample collection. We also thank Hua Zhang in National Institute of Advanced Industrial Science and Technology for technical support. We are grateful to Masao Sorai in National Institute of Advanced Industrial Science and Technology for helpful comments about changes in physicochemical conditions of the deep subsurface after CCS was carried out. This study was financially supported in part by JSPS KAKENHI Grant Numbers 22654066, 23244109, 23657069, 23681044, 24780089 and 25289333.

Author contributions

This study was designed by S.S. and H.M. The construction of the microcosms and the monitoring of gas compositions were performed by D.M., Y.M., and M.I. Analysis of carbon isotopic compositions was performed by D.M. and S.S. The 16S rRNA gene clone library and qPCR analyses were conducted by D.M. Thermodynamic calculations were performed by D.M. and J.D. The manuscript was written by D.M., H.T., J.D., S.S., M.T., C.H.N. and Y.K., assisted by all co-authors.

Additional information

Accession codes: All 16S rRNA gene sequences obtained in this study have been deposited at DDBJ under accession numbers AB668482–AB668513 and AB710350–AB710376.

Supplementary Information accompanies this paper at http://www.nature.com/naturecommunications

Competing financial interests: The authors declare no competing financial interests.

Reprints and permission information is available online at http://npg.nature.com/reprintsandpermissions/

How to cite this article: Mayumi, D. *et al.* Carbon dioxide concentration dictates alternative methanogenic pathways in oil reservoirs. *Nat. Commun.* 4:1998 doi: 10.1038/ncomms2998 (2013).